A DISPERSIVE APPROACH TO THE GIANT LOCALIZED CP VIOLATION IN $B^{\pm} \to K^{\pm}\pi^{+}\pi^{-}$*

Alba Reyes-Torrecilla [a,†], Christoph Hanhart [b]
Leon A. Heuser [c], Bastian Kubis [c], Patricia C. Magalhães [d]
Thomas Mannel [e], José R. Peláez [a]

[a]Departamento de Física Teórica and IPARCOS
Universidad Complutense de Madrid, 28040 Madrid, Spain
[b]Institute for Advanced Simulation (IAS-4), Forschungszentrum Jülich
52425 Jülich, Germany
[c]Helmholtz-Institut für Strahlen- und Kernphysik
and Bethe Center for Theoretical Physics, Universität Bonn
53115 Bonn, Germany
[d]Departamento de Raios Cósmicos e Cronologia
Universidade Estadual de Campinas 13083-860, Campinas, Brazil
[e]Center of Particle Physics (CPPS), Theoretische Physik 1, Universität Siegen
57068 Siegen, Germany

Received 4 April 2026, accepted 8 June 2026,
published online 10 July 2026

In this article, we review our recent dispersive analysis of the large localized CP-violating asymmetries observed by LHCb in $B^{\pm} \to K^{\pm}\pi^{+}\pi^{-}$ decays. Low-energy $\pi\pi$ final-state interactions are treated in a model-independent way, and the weak decay is described as a short-distance source. By fitting angular-projected data, we reproduce the Dalitz-plot CP-asymmetry pattern at low $m_{\pi\pi}$. Our framework highlights the essential role of the non-resonant isospin-2 S wave, ensures unitarity, and can be extended to other three-body decays.

DOI:10.5506/APhysPolBSupp.19.4-A21

1. Introduction

The study of CP violation (CPV) in non-leptonic heavy-meson decays provides a powerful probe of the flavor structure of the Standard Model (SM). In the SM, CPV originates from the complex phase of the Cabibbo–Kobayashi–Maskawa (CKM) matrix [1, 2] and arises through the interference

* Presented by A. Reyes-Torrecilla at the Excited QCD 2026 Workshop, Granada, Spain, 8–14 January, 2026.

† Corresponding author: albrey01@ucm.es

of amplitudes with different weak and strong phases. While two-body B decays can often be addressed within QCD factorization, three-body decays remain theoretically challenging due to the non-trivial role of strong final-state interactions (FSI) [3].

The LHCb Collaboration achieved a major experimental advance, measuring CP asymmetries in three-body B decays to three light mesons with unprecedented precision [4, 5]. Although integrated asymmetries are typically small, LHCb observed strikingly large CPV asymmetries, up to 60%, localized in specific regions of the Dalitz plot [6]. In $B^\pm \to K^\pm\pi^+\pi^-$ decays, most of those large asymmetries appear at low $\pi\pi$ invariant masses.

Conventional isobar analyses based on Breit–Wigner parameterizations can capture some qualitative features of the data, but they suffer from intrinsic limitations, including violations of unitarity, an inadequate treatment of non-resonant contributions, and the lack of a direct connection to $\pi\pi$ scattering data. This motivates the development of approaches that incorporate FSI in a model-independent and theoretically consistent way.

In this article, we summarize our recent dispersive analysis of $B^\pm \to K^\pm\pi^+\pi^-$ decays that addresses these challenges [7]. By exploiting the universality of low-energy $\pi\pi$ interactions and using dispersive parametrizations of the $\pi\pi$ amplitudes following [8], while neglecting three-body effects and retaining only two-body $\pi\pi$ final-state interactions, the framework provides a unitary and model-independent description of FSI and offers a description of the observed large localized CPV effects.

2. Dispersive treatment of FSI

The $B^\pm \to K^\pm\pi^+\pi^-$ decay is described by the Mandelstam variables $s = m^2_{\pi\pi}$ and $t = m^2_{K\pi}$, with $z = \cos\theta$, where θ is the angle between the kaon and one of the pions in the $\pi\pi$ rest frame. In the low-$m_{\pi\pi}$ region, the $\pi\pi$ system is dominated by a small set of partial waves: the isoscalar $S0$, containing the broad $f_0(500)$ and the narrow $f_0(980)$; the P wave, dominated by the $\rho(770)$ and including the effects of ρ–ω mixing, that we include analogously to [9]; and the non-resonant isotensor $S2$ wave. Higher partial waves are strongly suppressed and can be neglected.

Elastic unitarity relates the discontinuity of the production amplitude to the $\pi\pi$ scattering amplitude, leading to a solution in terms of Omnès functions [10], $\Omega_i(s)$,

$$\mathcal{A}_i^\pm(s) = P_i(s)\Omega_i(s)\bar{\mathcal{A}}_i^\pm\,, \tag{1}$$

where $i = S0_n$, $S0_s$, P, $S2$. Note here that, for the $S0$ wave, a coupled-channel $\pi\pi$–$K\bar{K}$ treatment is required due to the proximity of the $f_0(980)$ to the $K\bar{K}$ threshold, leading to both contributions $S0n$ and $S0s$. The Omnès functions are constructed from the $\pi\pi$ phase shifts and encode the

analytic structure of the hadron–hadron interactions. The polynomials $P_i(s)$ account for possible cross-channel and high-energy effects and are taken to be linear in s [9], whose slopes will be fit to LHCb data. The short-distance production is contained in the source terms $\bar{\mathcal{A}}_i^{\pm}$. This construction ensures exact two-body unitarity and automatically satisfies Watson's theorem in the elastic region [11].

3. Weak decay and source terms

The short-distance weak decay is governed by two contributions proportional to the CKM factors $V_{cb}V_{cs}^*$ and $V_{ub}V_{us}^*$ [12], corresponding to the two quark-level topologies shown in Fig. 1. In the standard CKM parameterization, only the latter, Fig. 1 (b), carries the weak CPV phase γ, while the former is CP-conserving. The corresponding hadronic matrix elements are treated as short-distance source terms for the $K\pi\pi$ final state.

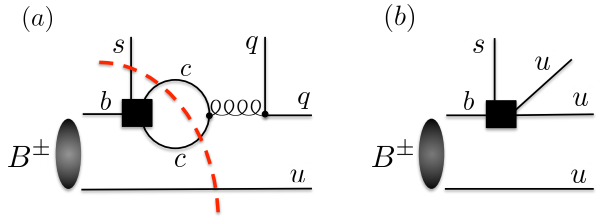

Fig. 1. Quark-level topologies for $B^+ \to K^+\pi^+\pi^-$ decays with (a) and without (b) a charm loop. The black box denotes the weak interaction carrying the CKM factors and CPV phase.

A key ingredient is the charm-loop topology shown in Fig. 1 (a). Its hadronization into intermediate hadronic states, such as $D\bar{D}$, generates CP-even strong phases once it couples to the light $\pi\pi$ system [13, 14]. These hadronization effects are not modeled explicitly but absorbed into complex source terms, which are not expected to yield strong energy dependencies, and thus they are approximated as constants.

For each $\pi\pi$ partial wave, the source terms are parametrized as follows:

$$\bar{A}_i^{\pm} = \hat{A}_i + e^{\pm i\gamma}\hat{B}_i \equiv a_i \pm ib_i + ic_i\,, \tag{2}$$

where $\hat{A}_i$ collects the CP-even contributions associated with the charm-loop topology, and $\hat{B}_i$ is real and encodes the CP-odd contribution. Since flavor and isospin symmetries reduce the number of independent parameters a_i, b_i and c_i, the fit contains thirteen real parameters.

4. CPV observables and results

The decay rates of B^+ and B^- define the CPV difference $\Delta\Gamma_{\rm CP}(s,z)$ and the CP-even sum $\Sigma\Gamma(s,z)$, from which the CP asymmetry $\mathcal{A}_{\rm CP}$ reads

$$\mathcal{A}_{\rm CP}(s,t) = \frac{\Delta\Gamma_{\rm CP}(s,z)}{\Sigma\Gamma(s,z)} = \frac{\Gamma^-(s,z) - \Gamma^+(s,z)}{\Gamma^-(s,z) + \Gamma^+(s,z)}\,. \tag{3}$$

The fit to these projections in the low-$m_{\pi\pi}$ region provides a good description of all data sets within uncertainties, reproducing the main features observed in the CPV distributions shown in Fig. 2. Higher partial waves or additional free parameters do not improve the fit, indicating that the dominant dynamics arises from the lowest S and P waves.

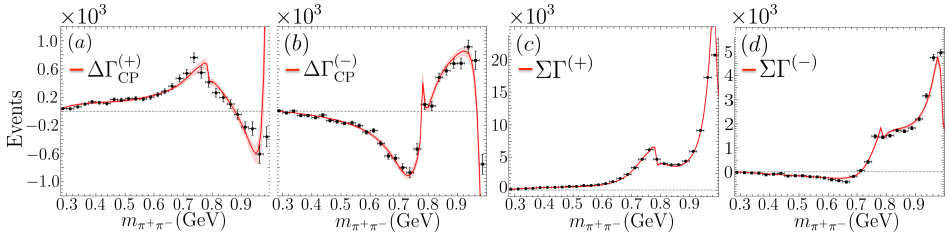

Fig. 2. Fit to the projected event distributions of the symmetric (+) and antisymmetric (−) combinations *versus* LHCb data [6] (supplemental material). We show (a) the angle-symmetric sum of yields, (b) the angle-asymmetric sum of yields, (c) the angle-symmetric CPV difference of yields, and (d) the angle-asymmetric CPV difference of yields.

The amplitude decomposition shown in Fig. 3 highlights the essential role of the non-resonant isospin-2 S wave, whose interference with the $S0$ and P waves is crucial to reproduce the observed CPV. This contribution is absent in previous theoretical analyses [15–18], including those of LHCb.

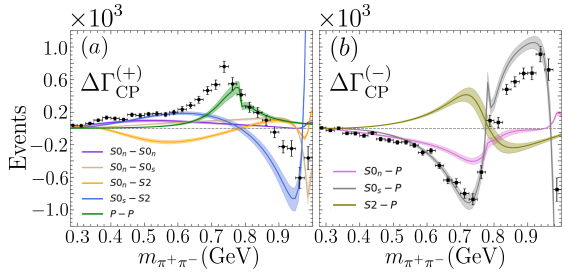

Fig. 3. (Color online) The most relevant contributions to the projected $\Delta\Gamma_{\rm CP}^{(\pm)}(s)$ distributions. Note isospin-2 S wave contributions in orange, blue, and olive, and P–P self-interference in green.

Strong phases from $c\bar{c}$ loop hadronization also play a key role, allowing for a P–P self-interference, which generates the pronounced peak observed in the CPV distributions in Fig. 3 (a).

Once the parameters are fixed, the framework predicts the full angular dependence of the decay amplitudes and the CP asymmetry over the Dalitz plot shown in Fig. 4 (b). The predicted distribution shows excellent agreement with the LHCb measurements in Fig. 4 (a), including the localized regions with giant CP asymmetries. In such regions, the CP-conserving denominator $\Sigma\Gamma$ in Fig. 4 (d) is very suppressed, and even a moderate contribution in the CPV numerator $\Delta\Gamma_{\rm CP}$ in Fig. 4 (c) can lead to a very large relative asymmetry. The large asymmetries are thus not driven by an exceptionally large absolute CPV difference, but rather by a strongly suppressed denominator.

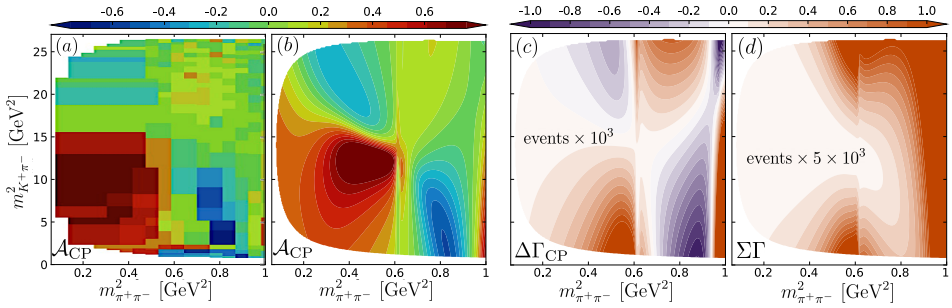

Fig. 4. $B^\pm \to K^\pm\pi^+\pi^-$ Dalitz plot section for $m^2_{\pi^+\pi^-} \leq 1$ GeV^2. (a) LHCb binned raw CP asymmetry $\mathcal{A}_{\rm CP}$, cropped and enlarged from Fig. 3 of Ref. [6]. (b) $\mathcal{A}_{\rm CP}$, Eq. (3) from our analysis. (c) CPV difference $\Delta\Gamma_{\rm CP}$ (numerator of Eq. (3)). (d) CP-conserving sum $\Sigma\Gamma$ (denominator in Eq. (3)).

5. Summary and conclusions

In this article, we have reviewed our recent dispersive analysis of the $B^\pm \to K^\pm\pi^+\pi^-$ decays that achieves a quantitative description of the large localized CP asymmetries observed experimentally. The key ingredients of the framework are a universal, model-independent treatment of low-energy $\pi\pi$ final-state interactions via Omnès functions and a parameterization of the weak decay source with a clear physical interpretation. The approach preserves unitarity and avoids the model dependence typical of traditional isobar analyses. Our results highlight the essential role of CP-odd strong phases arising from the hadronization of intermediate states, such as $D\bar{D}$ contributions from the $c\bar{c}$ loop shown in Fig. 1 (a), as well as non-resonant effects, particularly the isotensor $S2$ wave, in shaping the CP-violating structure of the Dalitz plot. Moreover, the framework can be readily extended to other three-body B-meson decays and to different kinematic regions.

This work is partially supported by the grant PID2022-136510NB-C31 funded by MCI/AEI/10.13039/501100011033. It was formulated and initiated during the preparations of the newly accepted Color meets Flavor cluster, funded by the German Research Foundation (DFG) under Germany's Excellence Strategy–EXC 3107–Project-ID 533766364. The financial support of the European Union's Horizon 2020 research and innovation program under grant agreement No. 824093 (STRONG2020), the CAS President's International Fellowship Initiative under grant No. 2025PD0087 is also gratefully acknowledged. We thank the organizers of the Excited QCD 2026 Workshop for the excellent environment for scientific discussion.

REFERENCES

[1] N. Cabibbo, *Phys. Rev. Lett.* **10**, 531 (1963).
[2] M. Kobayashi, T. Maskawa, *Prog. Theor. Phys.* **49**, 652 (1973).
[3] S. Kränkl, T. Mannel, J. Virto, *Nucl. Phys. B* **899**, 247 (2015).
[4] LHCb Collaboration (R. Aaij *et al.*), *Phys. Rev. Lett.* **111**, 101801 (2013).
[5] LHCb Collaboration (R. Aaij *et al.*), *Phys. Rev. Lett.* **112**, 011801 (2014).
[6] LHCb Collaboration (R. Aaij *et al.*), *Phys. Rev. D* **108**, 012008 (2023).
[7] L.A. Heuser *et al.*, *Phys. Rev. Lett.* **136**, 111901 (2026).
[8] J.R. Peláez, P. Rabán, J. Ruiz de Elvira, *Phys. Rev. D* **111**, 074003 (2025).
[9] J. T. Daub, C. Hanhart, B. Kubis, *J. High Energy Phys.* **2016**, 009 (2016).
[10] R. Omnès, *Nuovo Cim.* **8**, 316 (1958).
[11] K.M. Watson, *Phys. Rev.* **95**, 228 (1954).
[12] L. Wolfenstein, *Phys. Rev. Lett.* **51**, 1945 (1983).
[13] I. Bediaga, T. Frederico, P.C. Magalhães, *Phys. Lett. B* **806**, 135490 (2020).
[14] T. Mannel, K. Olschewsky, K.K. Vos, *J. High Energy Phys.* **2020**, 073 (2020).
[15] H. Simma, D. Wyler, *Phys. Lett. B* **272**, 395 (1991).
[16] B. El-Bennich *et al.*, *Phys. Rev. D* **79**, 094005 (2009); *Erratum ibid.* **83**, 039903 (2011).
[17] H.-Y. Cheng, C.-K. Chua, Z.-Q. Zhang, *Phys. Rev. D* **94**, 094015 (2016).
[18] D. Boito *et al.*, *Phys. Rev. D* **96**, 113003 (2017).